

Supporting Information for

Dual Functional Lipid Coating for Nanopillar-based Capture of Circulating Tumor Cells with High Purity and Efficiency

*Hsin-Ya Lou^{1#}, Wenting Zhao^{2#}, Lindsey Hanson^{1&}, Connie Zeng¹, Yi Cui^{2, 3}, Bianxiao Cui^{1, *}*

¹Department of Chemistry, Stanford University, 380 Roth Way, Stanford, California 94305, United States.

²Department of Materials Science and Engineering, Stanford University, 476 Lomita Mall, Stanford, California 94305, United States.

³Stanford Institute for Materials and Energy Sciences, SLAC National Accelerator Laboratory, 2575 Sand Hill Rd, Menlo Park, California 94025, United States.

*To whom correspondences should be addressed

*E-mail: bcui@stanford.edu.

& Current address: Materials Sciences Division, Lawrence Berkeley National Laboratory, 1 Cyclotron Rd, Berkeley, CA 94720

#These authors contribute equally to this work.

Table S1

The geometry of quartz nanopillar arrays:

Pillar Diameter (nm)	Pillar Spacing (μm)	Abbreviation
500	20	d500p20
700	20	d700p20
1000	20	d1000p20
500	10	d500p10
700	10	d700p10
1000	10	d1000p10
500	5	d500p5
700	5	d700p5
1000	5	d1000p5
500	3	d500p3
700	3	d700p3
1000	3	d1000p3

Table S2

The relative surface area of quartz nanopillar arrays (Pillar height: 1.05 μm)

Pillar Geometry	Calculated total surface area ($\mu\text{m}^2/\text{array}$)	Relative surface area
Flat	10000	1
d500p20	10041.23	1.004123
d700p20	10057.73	1.005773
d1000p20	10082.47	1.008247
d500p10	10164.93	1.016493
d700p10	10230.91	1.023091
d1000p10	10329.87	1.032987
d500p5	10659.73	1.065973
d700p5	10923.63	1.092363
d1000p5	11319.47	1.131947
d500p3	11832.6	1.18326
d700p3	12565.63	1.256563
d1000p3	13665.19	1.366519

Movie S1: FRAP of supported lipid bilayer

Movie S2: FRAP of SA-488 on supported lipid bilayer

Movie S3: Clustering of SA-488 beneath the captured MCF7 cells

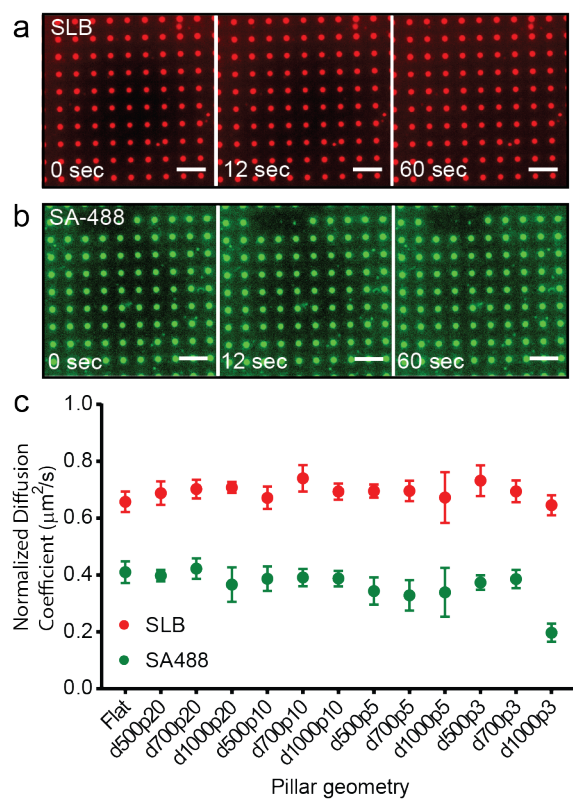


Figure S1. Fluidity of both the lipid molecules and streptavidin molecules on the supported lipid bilayers. **a-b.** FRAP experiment images of lipid (a) and SA-488 (b) on SLB formed on quartz nanopillars. Images were taken directly after bleaching (0sec). (Scale bars 5µm) **c.** Normalized diffusion coefficients of SLB and SA-488 on the SLB of all quartz nanopillar arrays. (Every experiment was repeated for 3 times (n = 3) and error bars represent the standard deviation (SD).)

Brightfield

SA-488

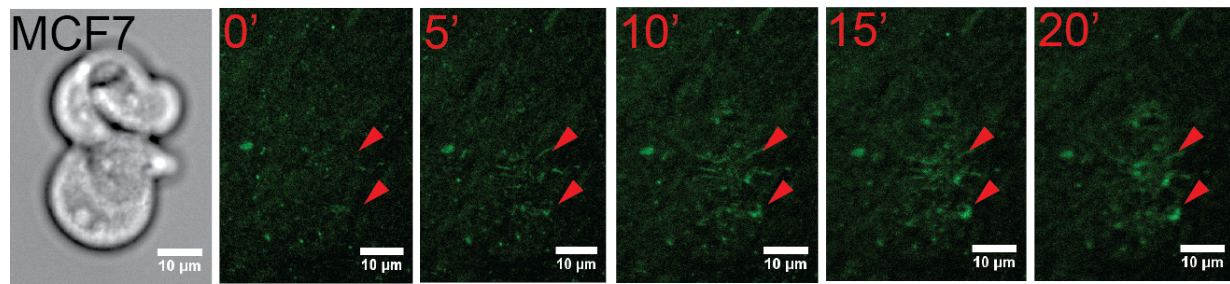


Figure S2. The clustering of anti-EpCAM formed beneath captured MCF7 cells on lipid-coated flat surface happened within 20-min incubation (indicated by red arrows).

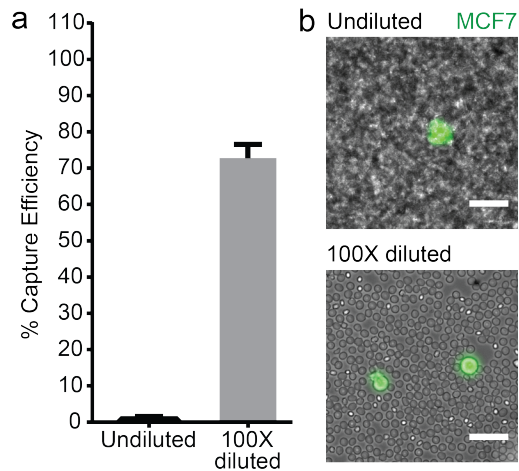


Figure S3. Capturing spiked MCF7 on lipid-coated quartz nanopillar arrays in undiluted and 100X diluted human whole blood. **a.** The capture efficiency of non-diluted blood is $0.6 \pm 1.0\%$, while using 100X diluted blood we could get capture efficiency of $72.8 \pm 3.8\%$. ($n=3$, the error bars represent standard deviation, SD) **b.** Blood cells and MCF7 cells (stained with Celcein-AM, green) on the anti-EpCAM functionalized support lipid bilayers. For undiluted blood, blood cells formed multi-layers on the SLB and overlapped with MCF7 cells. For 100X diluted blood, blood cells formed monolayer and had no overlap with MCF7 cells. (Scale bar $20 \mu\text{m}$)

MCF7

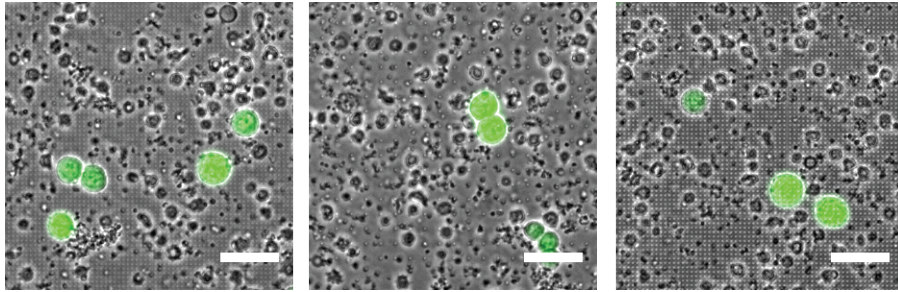


Figure S4. Three typical images of MCF7-spiked isolated PBMCs samples plated on lipid-coated quartz nanopillar arrays. It was showed that PBMCs had less or no overlap with MCF7 cells (stained with Celcein-AM, green). (Scale bar 40 μm)

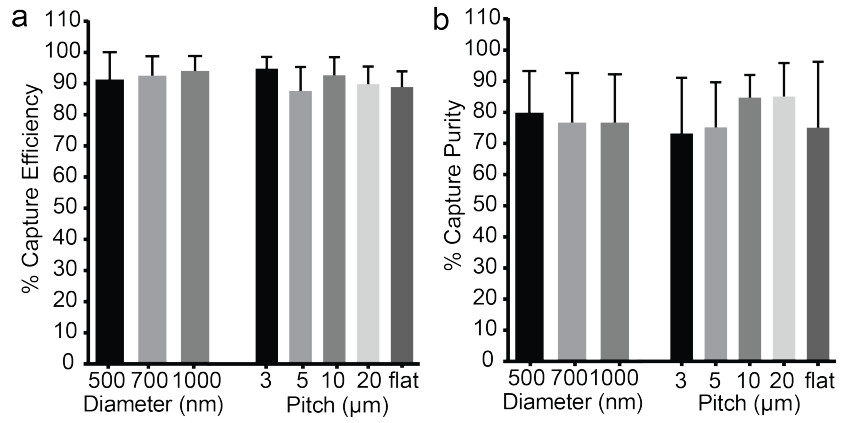


Figure S5. Capture efficiency (a) and capture purity (b) of spiked MCF7 cells in isolated PBMCs using quartz nanopillar arrays different diameters and pitches (n=6, the error bars represent standard deviation, SD).